where $V_{\rm BZ}$ is the volume of the BZ, the factor 2 accounts for the occupation with spin-up and spin-down electrons (in a non-spin-polarized case), and $\vartheta(\varepsilon - \varepsilon^j_{\mathbf{k}})$ is the step function, the value of which is 1 if $\varepsilon^j_{\mathbf{k}}$ is less than ε and 0 otherwise. The sum over $\mathbf{k}$ points has been replaced by an integral over the BZ, since the $\mathbf{k}$ points are uniformly distributed. Both expressions, sum and integral, are used in different derivations or applications. The Fermi energy is defined by imposing that $I(E_F) = N$, the number of (valence) electrons per unit cell.

The total DOS is defined as the energy derivative of $I(\varepsilon)$ as

$$n(\varepsilon) = \frac{{\rm d}I(\varepsilon)}{{\rm d}\varepsilon}, \qquad (2.2.14.2)$$

with the normalization

$$N = \int_{-\infty}^{E_F} n(\varepsilon)\ {\rm d}\varepsilon, \qquad (2.2.14.3)$$

where the integral is taken from $-\infty$ if all core states are included or from the bottom of the valence bands, often taken to be at zero. This defines the Fermi energy (note that the energy range must be consistent with N). In a bulk material, the origin of the energy scale is arbitrary and thus only relative energies are important. In a realistic case with a surface (*i.e.* a vacuum) one can take the potential at infinity as the energy zero, but this situation is not discussed here.

The total DOS $n(\varepsilon)$ can be decomposed into a partial (or projected) DOS by using information from the wavefunctions as described above in Section 2.2.14.3. If the charge corresponding to the wavefunction of an energy state is partitioned into contributions from the atoms, a site-projected DOS can be defined as $n^t(\varepsilon)$, where the superscript t labels the atom t. These quantities can be further decomposed into ℓ-like contributions within each atom to give $n^t_\ell(\varepsilon)$. As discussed above for the partial charges, a further partitioning of the ℓ-like terms according to the site symmetry (point group) can be done (in certain cases) by taking the proper m combinations, *e.g.* the t_{2g} and e_g manifold of the fivefold degenerate d orbitals in a octahedral ligand field. The latter scheme requires a local coordinate system in which the spherical harmonics are defined (see Section 2.2.13). In this context all considerations as discussed above for the partial charges apply again. Note in particular the difference between site-centred and spatially decomposed wavefunctions, which affects the partition of the DOS into its wavefunction-dependent contributions. For example, in atomic sphere representations as in LAPW we have the decomposition

$$n(\varepsilon) = n^{\rm out}(\varepsilon) + \sum_t \sum_\ell n^t_\ell(\varepsilon). \qquad (2.2.14.4)$$

In the case of spin-polarized calculations, one can also define a spin-projected DOS for spin-up and spin-down electrons.

2.2.15. Electric field gradient tensor

2.2.15.1. *Introduction*

The study of hyperfine interactions is a powerful way to characterize different atomic sites in a given sample. There are many experimental techniques, such as Mössbauer spectroscopy, nuclear magnetic and nuclear quadrupole resonance (NMR and NQR), perturbed angular correlations (PAC) measurements *etc.*, which access hyperfine parameters in fundamentally different ways. Hyperfine parameters describe the interaction of a nucleus with the electric and magnetic fields created by the chemical environment of the corresponding atom. Hence the resulting level splitting of the nucleus is determined by the product of a nuclear and an extra-nuclear quantity. In the case of quadrupole interactions, the nuclear quantity is the nuclear quadrupole moment (Q) that interacts with the electric field gradient (EFG) produced by the charges outside the nucleus. For a review see, for example, Kaufmann & Vianden (1979).

The EFG tensor is defined by the second derivative of the electrostatic potential V with respect to the Cartesian coordinates x_i, i = 1, 2, 3, taken at the nuclear site n,

$$\Phi_{ij} = \frac{\partial^2 V}{\partial x_i\ \partial x_j}\bigg|_n - \frac{1}{3}\delta_{ij}\nabla^2\bigg|_n, \qquad (2.2.15.1)$$

where the second term is included to make it a traceless tensor. This is more appropriate, since there is no interaction of a nuclear quadrupole and a potential caused by s electrons. From a theoretical point of view it is more convenient to use the spherical tensor notation because electrostatic potentials (the negative of the potential energy of the electron) and the charge densities are usually given as expansions in terms of spherical harmonics. In this way one automatically deals with traceless tensors (for further details see Herzig, 1985).

The analysis of experimental results faces two obstacles: (i) The nuclear quadrupole moments (Pyykkö, 1992) are often known only with a large uncertainty, as this is still an active research field of nuclear physics. (ii) EFGs depend very sensitively on the anisotropy of the charge density close to the nucleus, and thus pose a severe challenge to electronic structure methods, since an accuracy of the density in the per cent range is required.

In the absence of a better tool, a simple point-charge model was used in combination with so-called Sternheimer (anti-) shielding factors in order to interpret the experimental results. However, these early model calculations depended on empirical parameters, were not very reliable and often showed large deviations from experimental values.

In their pioneering work, Blaha *et al.* (1985) showed that the LAPW method was able to calculate EFGs in solids accurately without empirical parameters. Since then, this method has been applied to a large variety of systems (Schwarz & Blaha, 1992) from insulators (Blaha *et al.*, 1985), metals (Blaha *et al.*, 1988) and superconductors (Schwarz *et al.*, 1990) to minerals (Winkler *et al.*, 1996).

Several other electronic structure methods have been applied to the calculation of EFGs in solids, for example the LMTO method for periodic (Methfessl & Frota-Pessoa, 1990) or non-periodic (Petrilli & Frota-Pessoa, 1990) systems, the KKR method (Akai *et al.*, 1990), the DVM (discrete variational method; Ellis *et al.*, 1983), the PAW method (Petrilli *et al.*, 1998) and others (Meyer *et al.*, 1995). These methods achieve different degrees of accuracy and are more or less suitable for different classes of systems.

As pointed out above, measured EFGs have an intrinsic uncertainty related to the accuracy with which the nuclear quadrupole moment is known. On the other hand, the quadrupole moment can be obtained by comparing experimental hyperfine splittings with very accurate electronic structure calculations. This has recently been done by Dufek *et al.* (1995*a*) to determine the quadrupole moment of ^{57}Fe. Hence the calculation of accurate EFGs is to date an active and challenging research field.

2.2.15.2. *EFG conversion formulas*

The nuclear quadrupole interaction (NQI) represents the interaction of Q (the nuclear quadrupole moment) with the electric field gradient (EFG) created by the charges surrounding the nucleus, as described above. Here we briefly summarize the main ideas (following Petrilli *et al.*, 1998) and provide conversions between experimental NQI splittings and electric field gradients.

Let us consider a nucleus in a state with nuclear spin quantum number $I > 1/2$ with the corresponding nuclear quadrupole moment $Q_{i,j} = (1/e)\int {\rm d}^3 r \rho_n(r) r_i r_j$, where $\rho_n(r)$ is the nuclear

charge density around point **r** and e is the proton's charge. The interaction of this Q with an electric field gradient tensor $V_{i,j}$,

$$H = e\sum_{i,j} Q_{i,j}V_{i,j}, \tag{2.2.15.2}$$

splits the energy levels E_Q for different magnetic spin quantum numbers $m_I = I, I-1, \ldots, -I$ of the nucleus according to

$$E_Q = \frac{eQV_{zz}[3m_I^2 - I(I+1)](1+\eta^2/3)^{1/2}}{4I(2I-1)} \tag{2.2.15.3}$$

in first order of $V_{i,j}$, where Q represents the largest component of the nuclear quadrupole moment tensor in the state characterized by $m_I = I$. (Note that the quantum-mechanical expectation value of the charge distribution in an angular momentum eigenstate is cylindrical, which renders the expectation value of the remaining two components with half the value and opposite sign.) The conventional choice is $|V_{zz}| > |V_{yy}| \geq |V_{xx}|$. Hence, V_{zz} is the principal component (largest eigenvalue) of the electric field gradient tensor and the asymmetry parameter η is defined by the remaining two eigenvalues V_{xx}, V_{yy} through

$$\eta = \frac{|(V_{xx} - V_{yy})|}{|V_{zz}|}. \tag{2.2.15.4}$$

(2.2.15.3) shows that the electric quadrupole interaction splits the $(2I+1)$-fold degenerate energy levels of a nuclear state with spin quantum number I ($I > 1/2$) into I doubly degenerate substates (and one singly degenerate state for integer I). Experiments determine the energy difference Δ between the levels, which is called the quadrupole splitting. The remaining degeneracy can be lifted further using magnetic fields.

Next we illustrate these definitions for ^{57}Fe, which is the most common probe nucleus in Mössbauer spectroscopy measurements and thus deserves special attention. For this probe, the nuclear transition occurs between the $I = 3/2$ excited state and $I = 1/2$ ground state, with a 14.4 KeV γ radiation emission. The quadrupole splitting between the $m_I = \pm(1/2)$ and the $m_I = \pm(3/2)$ state can be obtained by exploiting the Doppler shift of the γ radiation of the vibrating sample.

$$\Delta = \frac{V_{zz}eQ(1+\eta^2/3)^{1/2}}{2}. \tag{2.2.15.5}$$

For systems in which the ^{57}Fe nucleus has a crystalline environment with axial symmetry (a threefold or fourfold rotation axis), the asymmetry parameter η is zero and Δ is given directly by

$$\Delta = \frac{V_{zz}eQ}{2}. \tag{2.2.15.6}$$

As η can never be greater than unity, the difference between the values of Δ given by equation (2.2.15.5) and equation (2.2.15.6) cannot be more than about 15%. In the remainder of this section we simplify the expressions, as is often done, by assuming that $\eta = 0$. As Mössbauer experiments exploit the Doppler shift of the γ radiation, the splitting is expressed in terms of the velocity between sample and detector. The quadrupole splitting can be obtained from the velocity, which we denote here by Δ_v, by

$$\Delta = \frac{E_\gamma}{c}\Delta_v, \tag{2.2.15.7}$$

where $c = 2.9979245580 \times 10^8$ m s^{-1} is the speed of light and $E_\gamma = 14.41 \times 10^3$ eV is the energy of the emitted γ radiation of the ^{57}Fe nucleus.

Finally, we still need to know the nuclear quadrupole moment Q of the Fe nucleus itself. Despite its utmost importance, its value has been heavily debated. Recently, however, Dufek *et al.* (1995*b*) have determined the value $Q = 0.16$ b for ^{57}Fe (1 b = 10^{-28} m^2) by comparing for fifteen different compounds theoretical V_{zz} values, which were obtained using the linearized augmented plane wave (LAPW) method, with the measured quadrupole splitting at the Fe site.

Now we relate the electric field gradient V_{zz} to the Doppler velocity *via*

$$\Delta_v = \frac{eQc}{2E_\gamma}V_{zz}. \tag{2.2.15.8}$$

In the special case of the ^{57}Fe nucleus, we obtain

$$V_{zz}\ [10^{21}\ \text{V m}^{-2}] = 10^4\frac{2E_\gamma\ [\text{eV}]}{c\ [\text{m s}^{-1}]Q\ [\text{b}]}\Delta_v\ [\text{mm s}^{-1}] \approx 6\Delta_v\ [\text{mm s}^{-1}]. \tag{2.2.15.9}$$

EFGs can also be obtained by techniques like NMR or NQR, where a convenient measure of the strength of the quadrupole interaction is expressed as a frequency ν_q, related to V_{zz} by

$$\nu_q = \frac{3eQV_{zz}}{2hI(2I-1)}. \tag{2.2.15.10}$$

The value V_{zz} can then be calculated from the frequency in MHz by

$$V_{zz}\ [10^{21}\ \text{V m}^{-2}] = 0.02771\frac{I(2I-1)}{Q\ [\text{b}]}\nu_q\ [\text{MHz}], \tag{2.2.15.11}$$

where $(h/e) = 4.1356692 \times 10^{-15}$ V Hz^{-1}. The principal component V_{zz} is also often denoted as $eq = V_{zz}$.

In the literature, two conflicting definitions of ν_q are in use. One is given by (2.2.15.10), and the other, defined as

$$\nu_q\ [\text{Hz}] = \frac{e^2qQ}{2h}, \tag{2.2.15.12}$$

differs from the first by a factor of 2 and assumes the value $I = 3/2$. Finally, the definition of $q = V_{zz}/e$ has been introduced here. In order to avoid confusion, we will refer here only to the definition given by (2.2.15.10). Furthermore, we also adopt the same sign convention for V_{zz} as Schwarz *et al.* (1990) because it has been found to be consistent with the majority of experimental results.

2.2.15.3. *Theoretical approach*

Since the EFG is a ground-state property that is uniquely determined by the charge density distribution (of electrons and nuclei), it can be calculated within DFT without further approximations. Here we describe the basic formalism to calculate EFGs with the LAPW method (see Section 2.2.12). In the LAPW method, the unit cell is divided into non-overlapping atomic spheres and an interstitial region. Inside each sphere the charge density (and analogously the potential) is written as radial functions $\rho_{LM}(r)$ times crystal harmonics (2.2.13.4) and in the interstitial region as Fourier series:

$$\rho(r) = \begin{cases} \sum_{LM}\rho_{LM}(r)K_{LM}(\hat{r}) & \text{inside sphere} \\ \sum_{K}\rho_K\exp(iKr) & \text{outside sphere} \end{cases} \tag{2.2.15.13}$$

The charge density coefficients $\rho_{LM}(r)$ can be obtained from the wavefunctions (KS orbitals) by (in shorthand notation)

$$\rho_{LM}(r) = \sum_{E_k^j < E_F}\sum_{\ell m}\sum_{\ell' m'} R_{\ell m}(r)R_{\ell' m'}(r)G_{L\ell\ell'}^{Mmm'}, \tag{2.2.15.14}$$

where $G_{L\ell\ell'}^{Mmm'}$ are Gaunt numbers (integrals over three spherical harmonics) and $R_{\ell m}(r)$ denote the LAPW radial functions [see (2.2.12.1)] of the occupied states E_k^j below the Fermi energy E_F. The dependence on the energy bands in $R_{\ell m}(r)$ has been omitted in order to simplify the notation.

For a given charge density, the Coulomb potential is obtained numerically by solving Poisson's equation in form of a boundary-value problem using a method proposed by Weinert (1981). This yields the Coulomb potential coefficients $v_{LM}(r)$ in analogy to (2.2.15.13) [see also (2.2.12.5)]. The most important contribution to the EFG comes from a region close to the nucleus of interest, where only the $L = 2$ terms are needed (Herzig, 1985). In the limit $r \to 0$ (the position of the nucleus), the asymptotic form of the potential $r^L v_{LM} K_{LM}$ can be used and this procedure yields (Schwarz *et al.*, 1990) for $L = 2$:

$$V_{2M} = -C_{2M} \int_0^R \frac{\rho_{2M}(r)}{r^3} r^2 \, \mathrm{d}r + C_{2M} \int_0^R \frac{\rho_{2M}(r)}{r} \left(\frac{r}{R}\right)^5 \mathrm{d}r + 5 \frac{C_{2M}}{R^2} \sum_K V(K) j_2(KR) K_{2M}(K), \quad (2.2.15.15)$$

with $C_{2M} = 2\sqrt{4\pi/5}$, $C_{22} = \sqrt{3/4} C_{20}$ and the spherical Bessel function j_2. The first term in (2.2.15.15) (called the *valence* EFG) corresponds to the integral over the respective atomic sphere (with radius R). The second and third terms in (2.2.15.15) (called the *lattice* EFG) arise from the boundary-value problem and from the charge distribution outside the sphere considered. Note that our definition of the lattice EFG differs from that based on the point-charge model (Kaufmann & Vianden, 1979). With these definitions the tensor components are given as

$$\begin{aligned} V_{xx} &= C\left[V_{22+} - \left(1/\sqrt{3}\right) V_{20}\right] \\ V_{yy} &= C\left[-V_{22+} - \left(1/\sqrt{3}\right) V_{20}\right] \\ V_{zz} &= C\left(2/\sqrt{3}\right) V_{20} \\ V_{xy} &= C V_{22-} \\ V_{xz} &= C V_{21+} \\ V_{yz} &= C V_{21-} \end{aligned} \quad (2.2.15.16)$$

where $C = \sqrt{15/4\pi}$ and the index M combines m and the partity p (*e.g.* 2+). Note that the prefactors depend on the normalization used for the spherical harmonics.

The non-spherical components of the potential v_{LM} come from the non-spherical charge density ρ_{LM}. For the EFG only the $L = 2$ terms (in the potential) are needed. If the site symmetry does not contain such a non-vanishing term (as for example in a cubic system with $L = 4$ in the lowest LM combination), the corresponding EFG vanishes by definition. According to the Gaunt numbers in (2.2.15.14) only a few non-vanishing terms remain (ignoring f orbitals), such as the p–p, d–d or s–d combinations (for f orbitals, p–f and f–f would appear), where this shorthand notation denotes the products of the two radial functions $R_{\ell m}(r) R_{\ell' m'}(r)$. The s–d term is often small and thus is not relevant to the interpretation. This decomposition of the density can be used to partition the EFG (illustrated for the V_{zz} component),

$$V_{zz} \approx V_{zz}^p + V_{zz}^d + \text{small contributions}, \quad (2.2.15.17)$$

where the superscripts p and d are a shorthand notation for the product of two p- or d-like functions.

Table 2.2.15.1. *Partial O 2p charges (in electrons) and electric field gradient tensor O EFG (in 10^{21} V m^{-2}) for $YBa_2Cu_3O_7$*

Numbers in bold represent the main deviation from spherical symmetry in the 2p charges and the related principal component of the EFG tensor.

Atom	p_x	p_y	p_z	V_{aa}	V_{bb}	V_{cc}
O1	1.18	**0.91**	1.25	−6.1	**18.3**	−12.2
O2	**1.01**	1.21	1.18	**11.8**	−7.0	−4.8
O3	1.21	**1.00**	1.18	−7.0	**11.9**	−4.9
O4	1.18	1.19	**0.99**	−4.7	−7.0	**11.7**

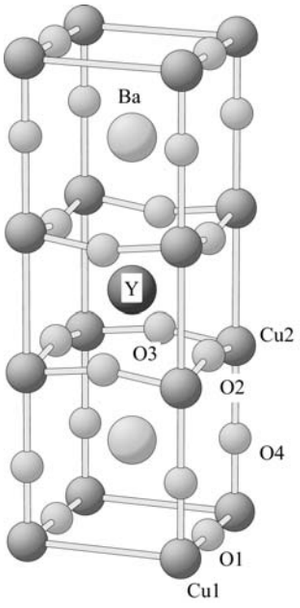

Fig. 2.2.15.1. Unit cell of the high-temperature superconductor $YBa_2Cu_3O_7$ with four non-equivalent oxygen sites.

From our experience we find that the first term in (2.2.15.15) is usually by far the most important and often a radial range up to the first node in the corresponding radial function is all that contributes. In this case the contribution from the other two terms is rather small (a few per cent). For first-row elements, however, which have no node in their 2p functions, this is no longer true and thus the first term amounts only to about 50–70%.

In some cases interpretation is simplified by defining a so-called asymmetry count, illustrated below for the oxygen sites in $YBa_2Cu_3O_7$ (Schwarz *et al.*, 1990), the unit cell of which is shown in Fig. 2.2.15.1.

In this case essentially only the O 2p orbitals contribute to the O EFG. Inside the oxygen spheres (all taken with a radius of 0.82 Å) we can determine the partial charges q_i corresponding to the p_x, p_y and p_z orbitals, denoted in short as p_x, p_y and p_z charges.

With these definitions we can define the p-like asymmetry count as

$$\Delta n_p = \tfrac{1}{2}(p_x + p_y) - p_z \quad (2.2.15.18)$$

and obtain the proportionality

$$V_{zz} \propto \left\langle 1/r^3 \right\rangle_p \Delta n_p, \quad (2.2.15.19)$$

where $\left\langle 1/r^3 \right\rangle_p$ is the expectation value taken with the p orbitals. A similar equation can be defined for the d orbitals. The factor $1/r^3$ enhances the EFG contribution from the density anisotropies close to the nucleus. Since the radial wavefunctions have an asymptotic behaviour near the origin as r^ℓ, the p orbitals are more sensitive than the d orbitals. Therefore even a very small p anisotropy can cause an EFG contribution, provided that the asymmetry count is enhanced by a large expectation value.

Often the anisotropy in the p_x, p_y and p_z occupation numbers can be traced back to the electronic structure. Such a physical interpretation is illustrated below for the four non-equivalent oxygen sites in $YBa_2Cu_3O_7$ (Table 2.2.15.1). Let us focus first on O1, the oxygen atom that forms the linear chain with the Cu1 atoms along the b axis. In this case, the p_y orbital of O1 points towards Cu1 and forms a covalent bond, leading to bonding and antibonding states, whereas the other two p orbitals have no bonding partner and thus are essentially nonbonding. Part of the corresponding antibonding states lies above the Fermi energy

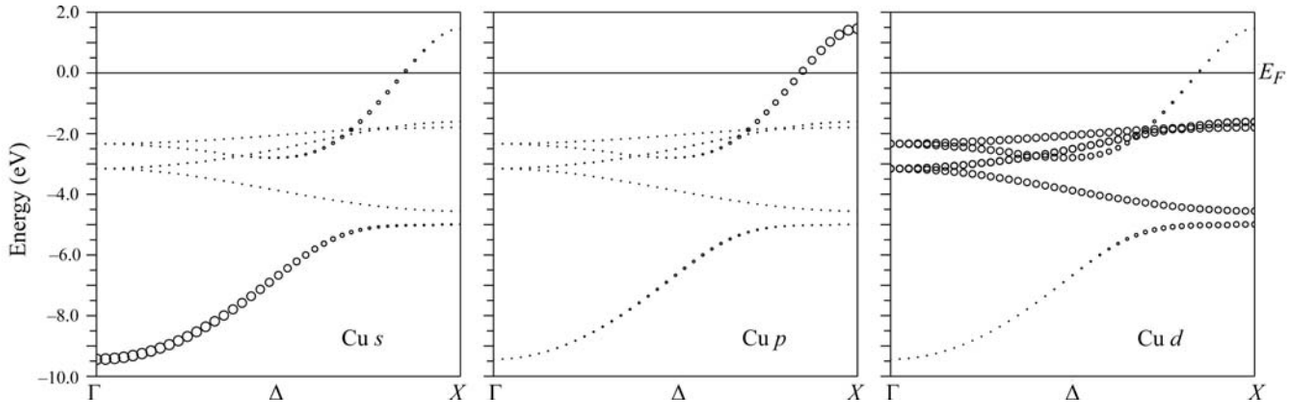

Fig. 2.2.16.1. Character of energy bands of f.c.c. copper in the Δ direction. The radius of each circle is proportional to the respective partial charge of the given state.

and thus is not occupied, leading to a smaller p_z charge of 0.91 e, in contrast to the fully occupied nonbonding states with occupation numbers around 1.2 e. (Note that only a fraction of the charge stemming from the oxygen 2*p* orbitals is found inside the relatively small oxygen sphere.) This anisotropy causes a finite asymmetry count [(2.2.15.18)] that leads – according to (2.2.15.19) – to a corresponding EFG.

In this simple case, the anisotropy in the charge distribution, given here by the different *p* occupation numbers, is directly proportional to the EFG, which is given with respect to the crystal axes and is thus labelled V_{aa}, V_{bb} and V_{cc} (Table 2.2.15.1). The principal component of the EFG is in the direction where the *p* occupation number is smallest, *i.e.* where the density has its highest anisotropy. The other oxygen atoms behave very similarly: O2, O3 and O4 have a near neighbour in the *a*, *b* and *c* direction, respectively, but not in the other two directions. Consequently, the occupation number is lower in the direction in which the bond is formed, whereas it is normal (around 1.2 e) in the other two directions. The principal axis falls in the direction of the low occupation. The higher the anisotropy, the larger the EFG (compare O1 with the other three oxygen sites). Excellent agreement with experiment is found (Schwarz *et al.*, 1990). In a more complicated situation, where *p* and *d* contributions to the EFG occur [see (2.2.15.17)], which often have opposite sign, the interpretation can be more difficult [see *e.g.* the copper sites in $YBa_2Cu_3O_7$; Schwarz *et al.* (1990)].

The importance of semi-core states has been illustrated for rutile, where the proper treatment of 3*p* and 4*p* states is essential to finding good agreement with experiment (Blaha *et al.*, 1992). The orthogonality between ℓ-like bands belonging to different principal quantum numbers (3*p* and 4*p*) is important and can be treated, for example, by means of local orbitals [see (2.2.12.4)].

In many simple cases, the off-diagonal elements of the EFG tensor vanish due to symmetry, but if they don't, diagonalization of the EFG tensor is required, which defines the orientation of the principal axis of the tensor. Note that in this case the orientation is given with respect to the local coordinate axes (see Section 2.2.13) in which the *LM* components are defined.

2.2.16. Examples

The general concepts described above are used in many band-structure applications and thus can be found in the corresponding literature. Here only a few examples are given in order to illustrate certain aspects.

2.2.16.1. *F.c.c. copper*

For the simple case of an element, namely copper in the f.c.c. structure, the band structure is shown in Fig. 2.2.16.1 along the Δ symmetry direction from Γ to *X*. The character of the bands can be illustrated by showing for each band state the crucial information that is contained in the wavefunctions. In the LAPW method (Section 2.2.12), the wavefunction is expanded in atomic like functions inside the atomic spheres (partial waves), and thus a spatial decomposition of the associated charge and its portion of ℓ-like charge (*s*-, *p*-, *d*-like) inside the Cu sphere, $q_\ell^{Cu}(E_{\mathbf{k}}^j)$, provides such a quantity. Fig. 2.2.16.1 shows for each state $E_{\mathbf{k}}^j$ a circle the radius of which is proportional to the ℓ-like charge of that state. The band originating from the Cu 4*s* and 4*p* orbitals shows an approximately free-electron behaviour and thus a k^2 energy dependence, but it hybridizes with one of the *d* bands in the middle of the Δ direction and thus the ℓ-like character changes along the Δ direction.

This can easily be understood from a group-theoretical point of view. Since the *d* states in an octahedral environment split into the e_g and t_{2g} manifold, the *d* bands can be further partitioned into the two subsets as illustrated in Fig. 2.2.16.2. The *s* band ranges from about −9.5 eV below E_F to about 2 eV above. In the Δ direction, the *s* band has Δ_1 symmetry, the same as one of the *d* bands from the e_g manifold, which consists of Δ_1 and Δ_2. As a consequence of the 'non-crossing rule', the two states, both with Δ_1 symmetry, must split due to the quantum-mechanical interaction between states with the same symmetry. This leads to the avoided crossing seen in the middle of the Δ direction (Fig. 2.2.16.1). Therefore the lowest band starts out as an '*s* band' but ends near *X* as a '*d* band'. This also shows that bands belonging to different irreducible representations (small representations) may cross. The fact that Γ_{12} splits into the subgroups Δ_1 and Δ_2 is an example of the compatibility relations. In addition, group-theoretical arguments can be used (Altmann, 1994) to show that in certain symmetry directions the bands must enter the face of the BZ with zero slope.

Note that in a site-centred description of the wavefunctions a similar ℓ-like decomposition of the charge can be defined as $1 = \sum_t \sum_\ell q_\ell^t$ (without the q^{out} term), but here the partial charges have a different meaning than in the spatial decomposition. In one case (*e.g.* LAPW), q_ℓ^t refers to the partial charge of ℓ-like character inside sphere *t*, while in the other case (LCAO), it means ℓ-like charge coming from orbitals centred at site *t*. For the main components (for example Cu *d*) these two procedures will give roughly similar results, but the small components have quite a different interpretation. For this purpose consider an orbital that is centred on the neighbouring site *j*, but whose tail enters the atomic sphere *i*. In the spatial representation this tail coming from the *j* site must be represented by the (*s*, *p*, *d etc.*) partial waves inside sphere *i* and consequently will be associated with site *i*, leading to a small partial charge component. This situation is sometimes called the off-site component, in contrast to the on-site component, which